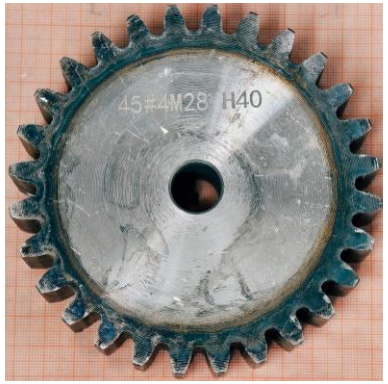

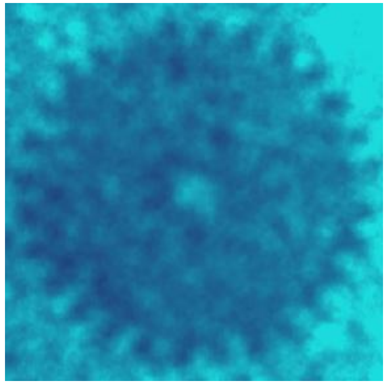

Millimeter-Resolution Cosmic-Ray Imaging via Projection-shifted MUon transMission tomogrAphy (PμMA)

arXiv:2512.19747

Zibo Qin

(on behalf of the PKMu Collaboration)

School of Physics, Peking University

2026/4/26, Huizhou, China

Introduction-MST

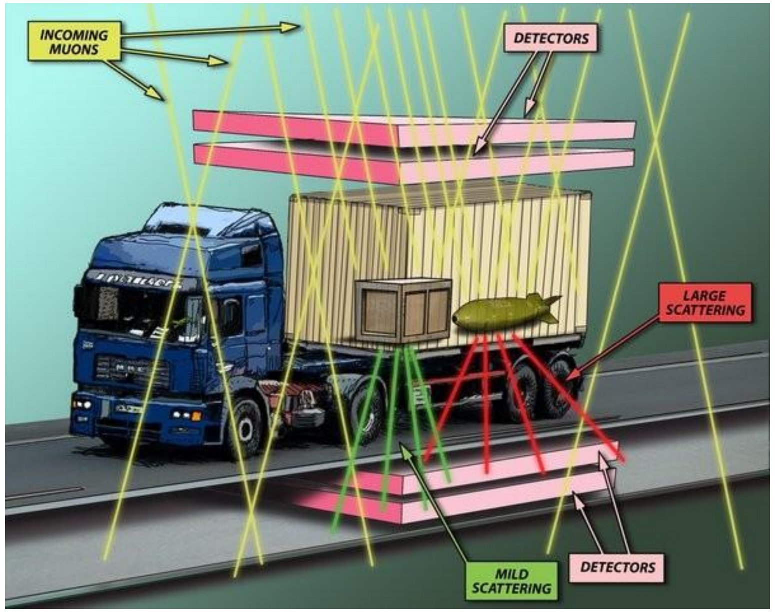

Muon Scattering Tomography (MST)

- Measuring the multiple Coulomb scattering (MCS) information of muons.
- Applied for nuclear security and safeguards (detecting shielded nuclear materials), cargo scanning, infrastructure inspection.
- Usually suitable for high-Z materials with limited resolution (~cm).

Can we do better?

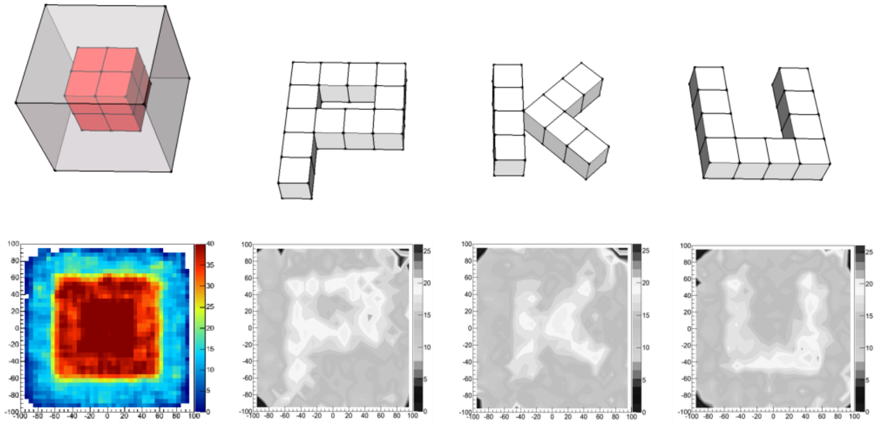

Our previous MST results

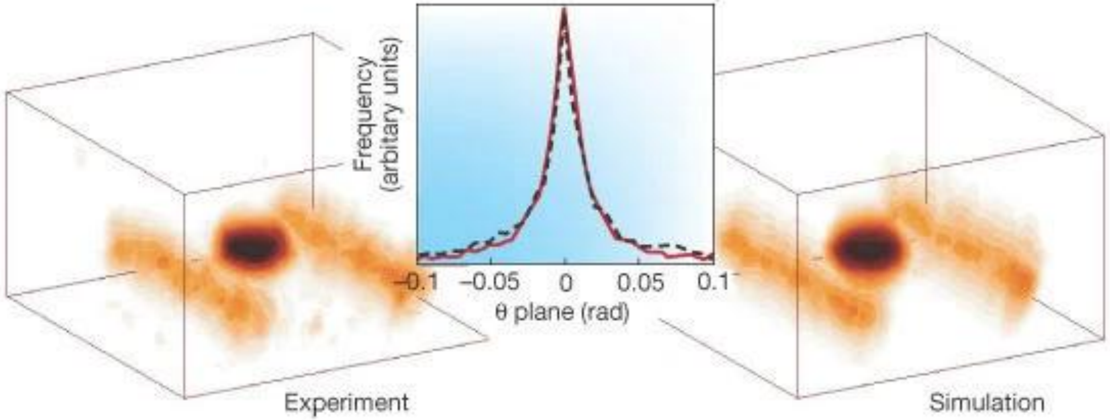

Nature 422, 277 (2003)
the beginning of MST

Introduction-PoCA

The Point of Closest Approach (PoCA) Algorithm

The fundamental algorithm for MST is PoCA. This algorithm approximates multiple Coulomb scattering as a single scattering process, and reconstructs the scattering angle and position (the PoCA point) based on the incoming and outgoing tracks.

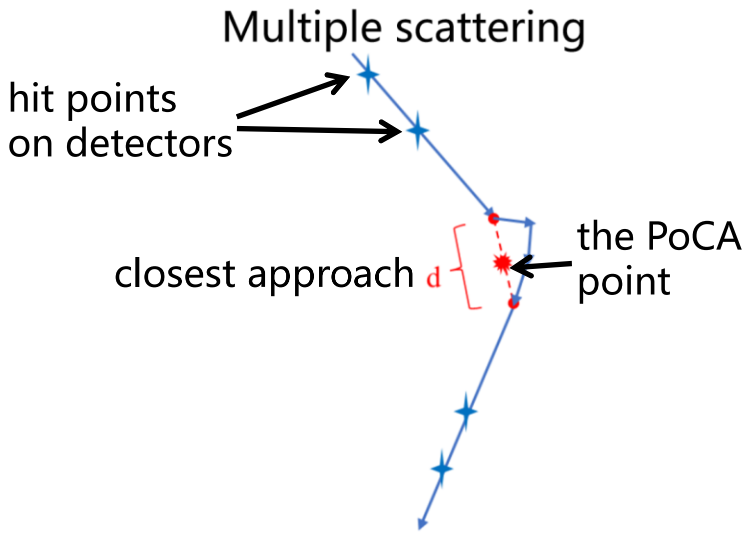

MST cannot utilize transmission (or absorption) information. Furthermore, due to the complexity of multiple scattering, the localization of the scattering position is not very accurate, especially when the scattering angle is small.

The PμMA Methods

Projection-shifted MUon transMission tomogrAphy (PμMA)

What is different?

- Transmission based
  (identify materials by transmission ratio)
- Transmission track by linear fit
  (accurate for mild scattering)
- Scattering information assistance
  (a scattering-induced lateral displacement)
- Background required
  (to eliminate non-uniformity by detector geometry)

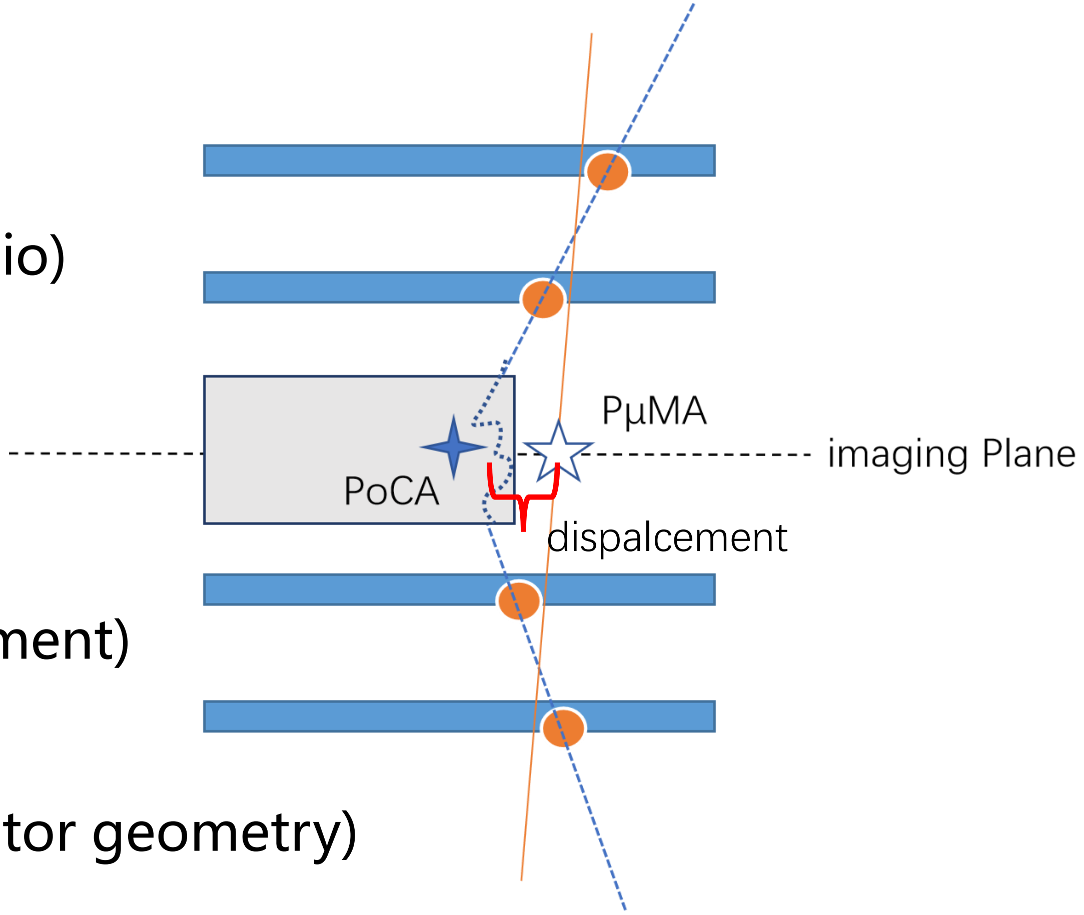

*The imaging plane is a plane set at the approximate height of the sample. PμMA locates the intersection point of the transmission track with this plane.

The PμMA Methods

The Shifted Projection

We recognize a scattering-induced displacement, denoted as D, between the reconstructed and real transmission points on the imaging plane. It is a shifted projection of muon track on the imaging plane.

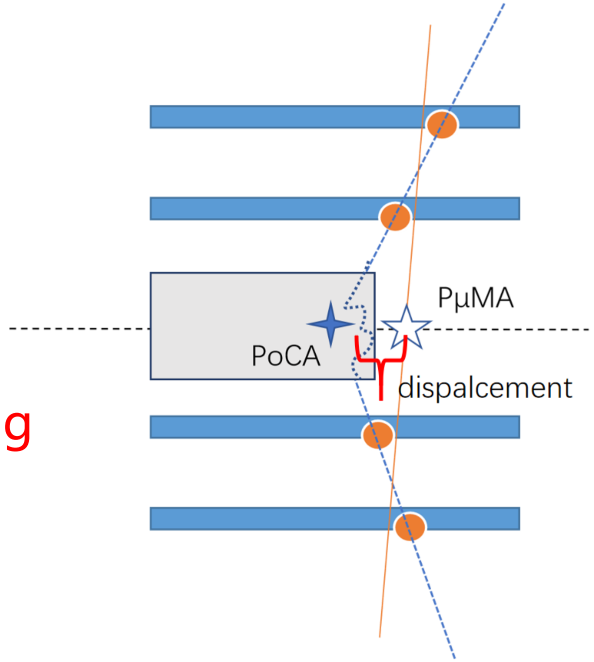

Considering a one-dimensional case (an infinite straight boundary), the displacement distribution D(x) within two different material regions (e.g., air and lead) can be expressed respectively as:

$$D_{air}(x) = \alpha \cdot f(x), D_{lead}(x) = \beta \cdot g(x)$$

where α and β are transmissivities, and f(x) and g(x) are normalized even functions. We expect D_{air} to be narrow and steep, and D_{lead} to be wide and flat.

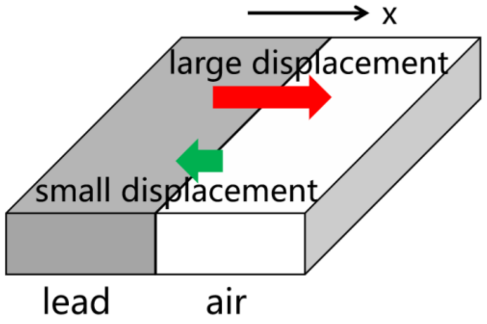

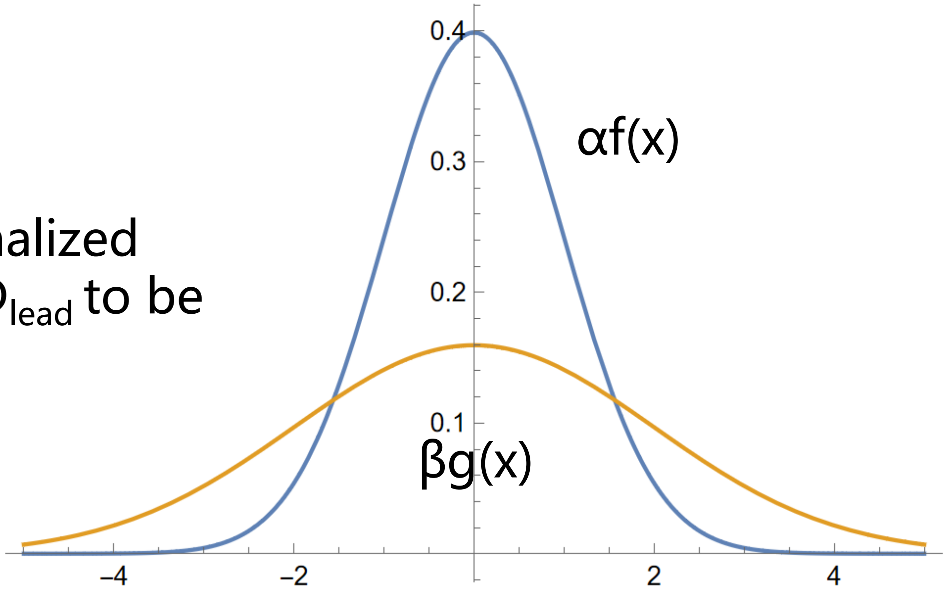

D(x) sketch map

MCS Scattering angle distribution:

$$\sigma_\theta = \frac{13.6\mathrm{MeV}}{\beta cp} z \sqrt{\frac{x}{X_0}} \left[1 + 0.038 \ln\left(\frac{xz^2}{X_0 \beta^2}\right)\right]$$

The PμMA Methods

The Edge Spread Function (ESF)

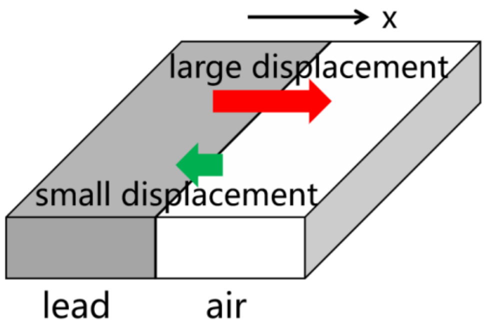

The transmission ratio (TR) then can be written as

$$TR(x) = \beta + \int_0^{+\infty} [\alpha f - \beta g](x - x')dx'.$$

TR(x) can also be regarded as an edge spread function (ESF), the blurred image of an ideal step change (like a knife edge).

The edge spread (distance between the red points) can be considered similar to the broadening of D_{air}. Our advantage

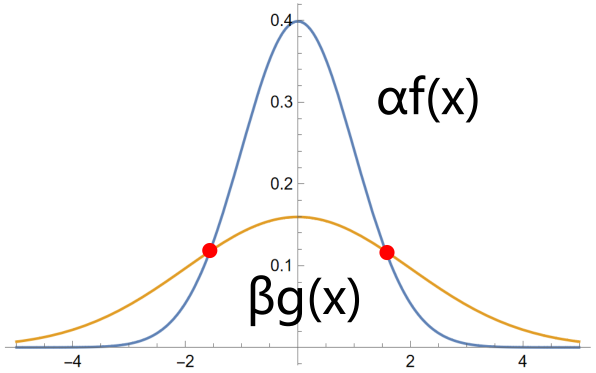

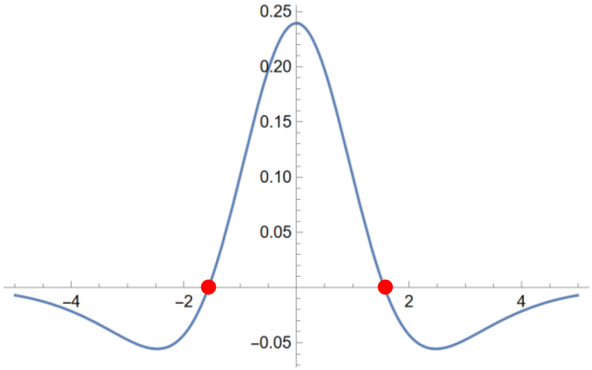

αf(x)-βg(x)

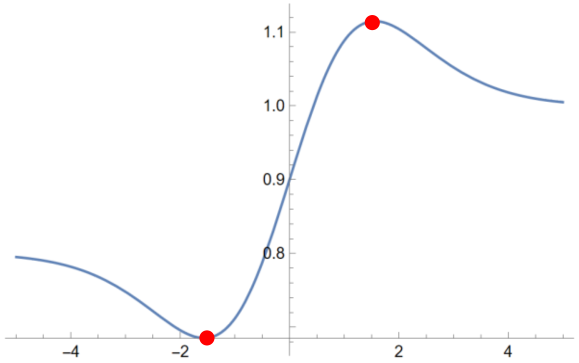

TR(x)

The PμMA Methods

PμMA2--Lightweight and Rapid Method

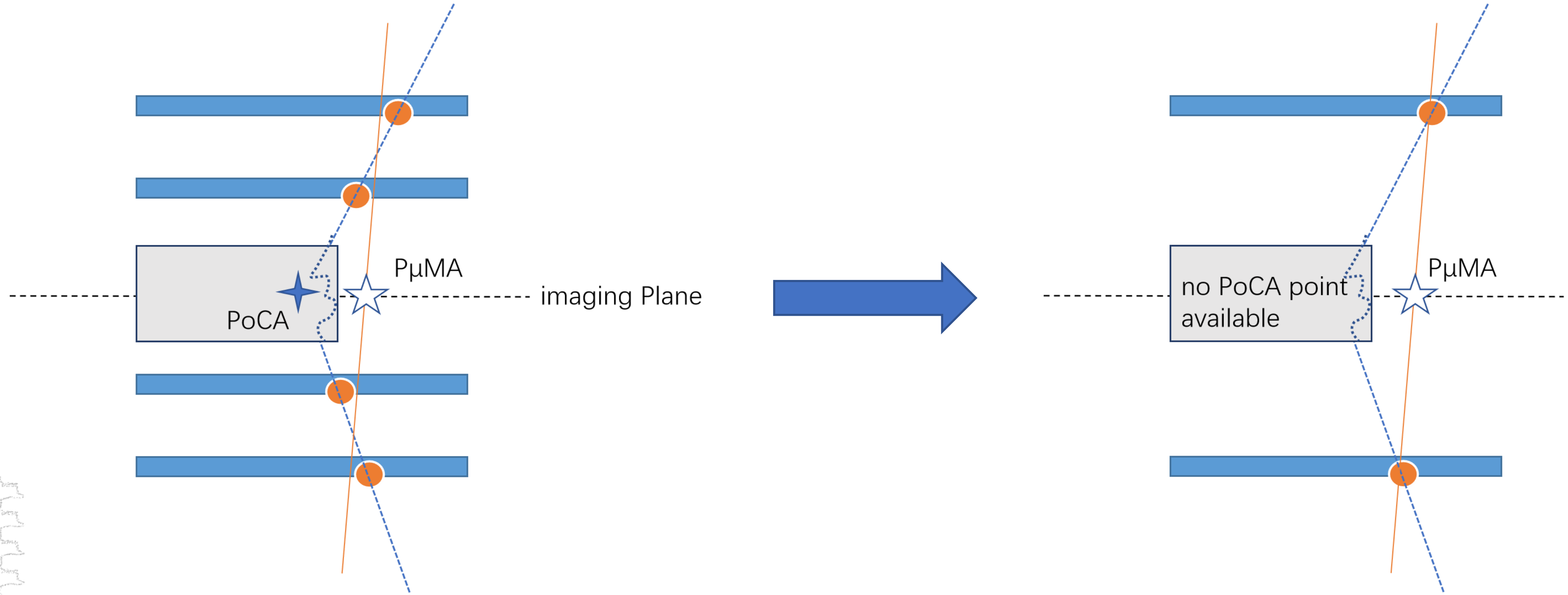

No need to reconstruct the scattering!

The PμMA Methods

PμMAC -- A Variant

A variant of PμMA, called PμMAC, introduces a scattering angle threshold; events exceeding this threshold are treated as non-transmitting.

From the perspective of the Edge Spread Function (ESF), this constraint brings the broadening of D(x) in different regions to nearly the same level, while making the difference in transmissivity (α, β) more pronounced.

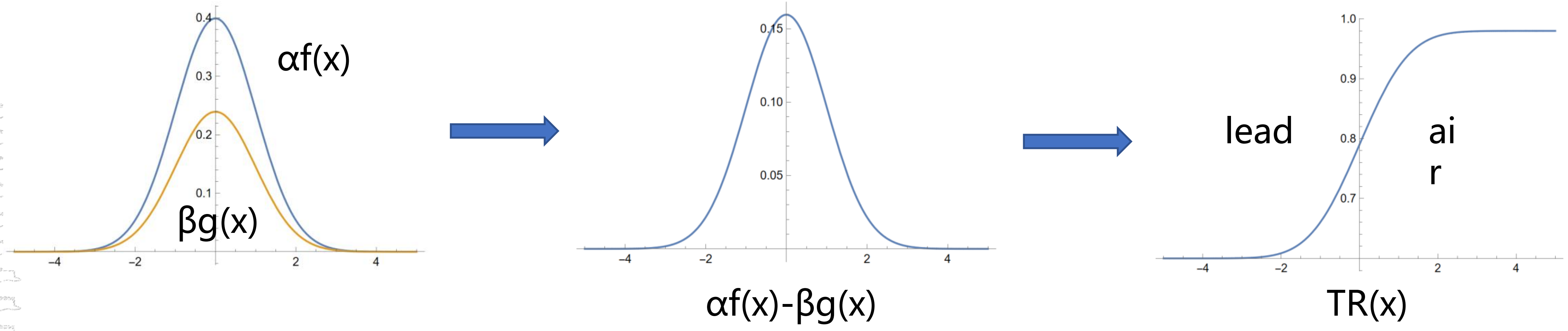

Simulation Results & Evaluation

Air-Lead Boundary Simulation

The cosmic-ray imaging simulation was implemented using the CRY package in GEANT4, with approximately 50 million events. The sample is a 3 cm thick lead block in the shape of a parallelogram, with a hypotenuse of 240 mm and a side length of 120 mm.

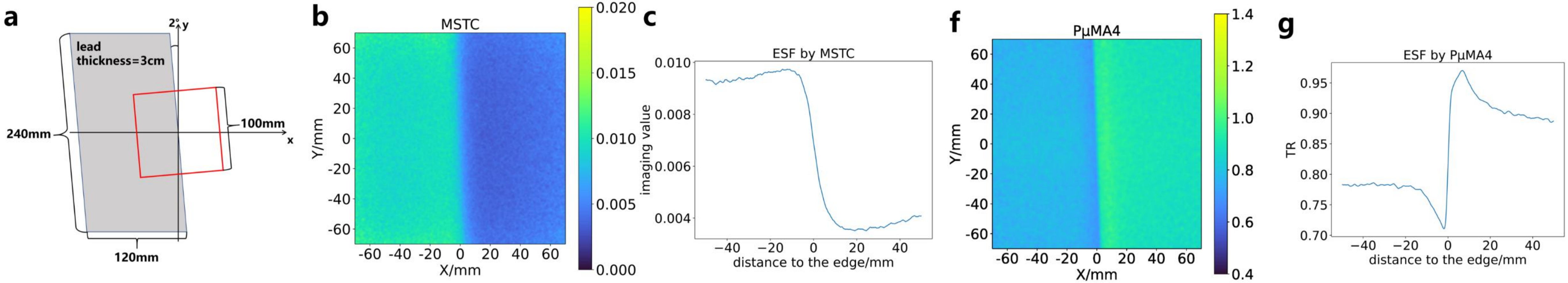

*PμMA4 means the number of RPCs for imaging is 4.
*MSTC is an optimized muon scattering tomography (MST).
See NIMA 1069, 169932 (2024).

Simulation Results & Evaluation

Air-Lead Boundary Simulation

A simulation under ideal conditions: a monoenergetic collimated muon beam with an energy of 4 GeV, without considering the effects of detector position resolution. The number of events is approximately 10 million for PμMA4 and 50 million for PμMA2.

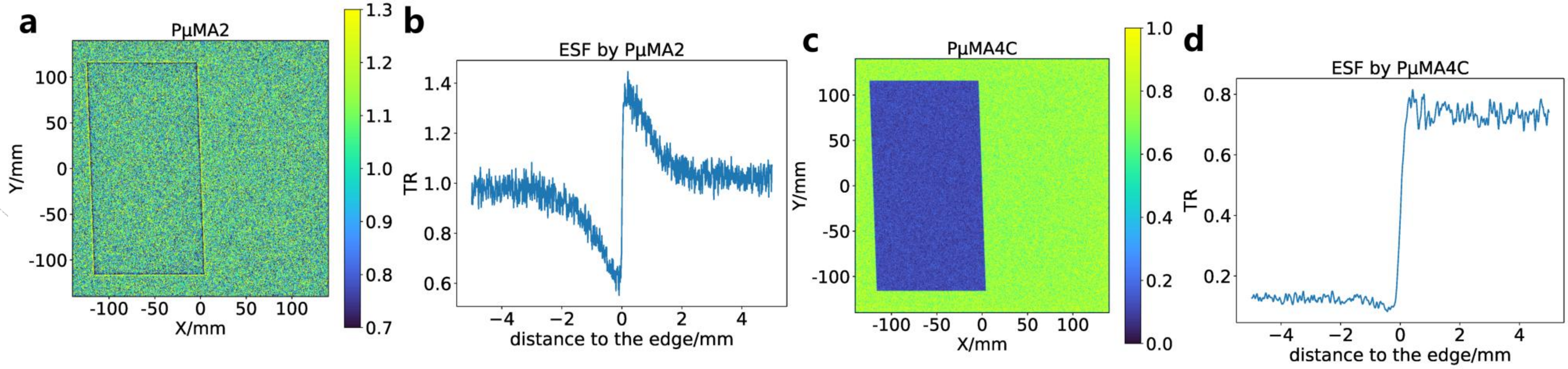

Simulation Results & Evaluation

Knife-edge Width

Inspired by the concept of rise time in electronic signals, the width between the 20% and 80% points of the ESF "rise" is defined as the knife-edge width of the ESF.

The table below lists some measured knife-edge widths of the PμMA methods in simulated imaging at an air-lead boundary. The advantage of PμMA is obvious.

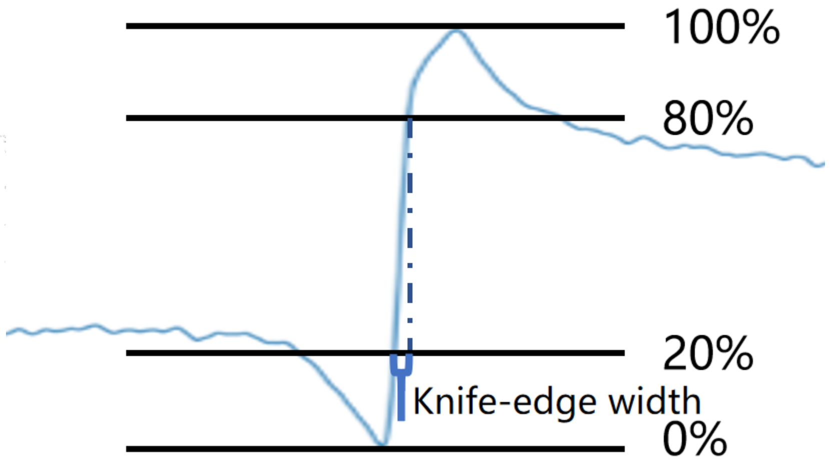

Method	Knife-edge Width/mm
MSTC	7.242±0.112
PμMA2	2.128±0.108
PμMA4	1.732±0.028

Ideal Muon Beam:
PμMA2 48μm
PμMA4 238μm

Experimental Results

Our detection system

Setup

We used self-developed Resistive Plate Chambers (RPCs) as muon detectors. Each RPC has

- a sensitive area of 28 cm × 28 cm;
- an optimal position resolution of 0.5–0.7 mm (σ);
- a detection efficiency of over 80%.

A typical 4-RPC cosmic-ray muon detection system is shown in the left figure, with inter-layer spacings of approximately 20 cm, 50 cm, and 20 cm from top to bottom. This system has already been used for muon imaging experiments and potential muonphilic dark matter detection experiments (Phys. Rev. Lett. 136, 151001, published 2026).

Experimental Results

Experimental Imaging Results 1 -- Copper Letters

How can we identify copper-made letters with cosmic ray?

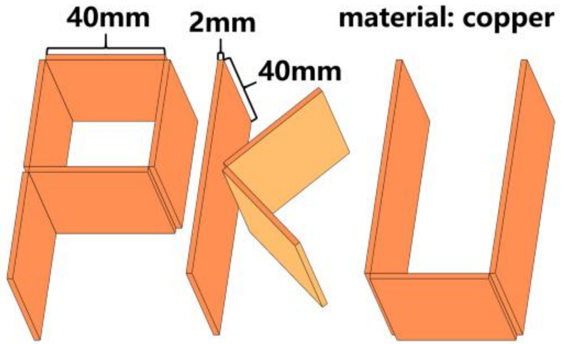

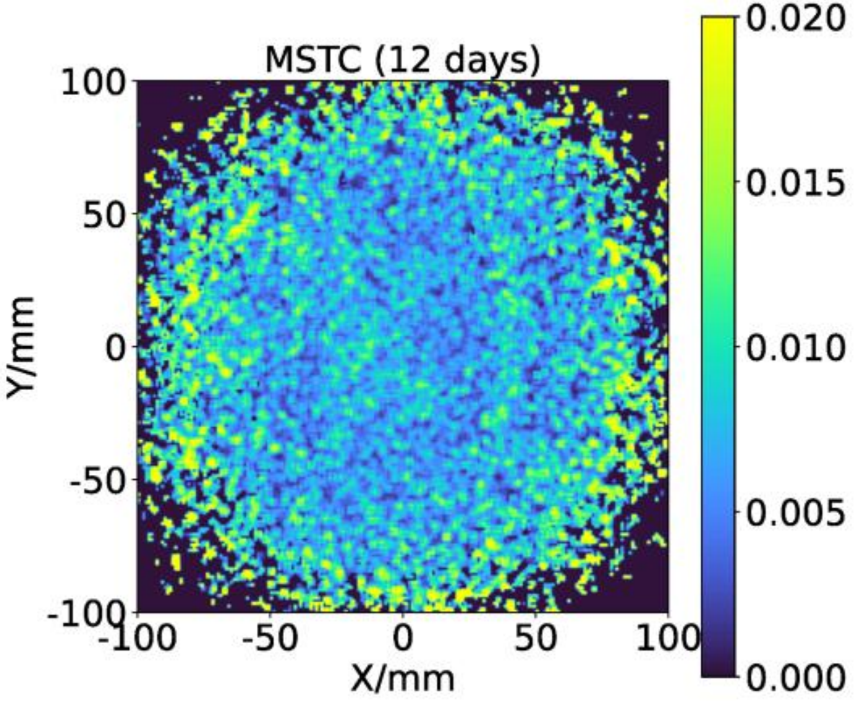

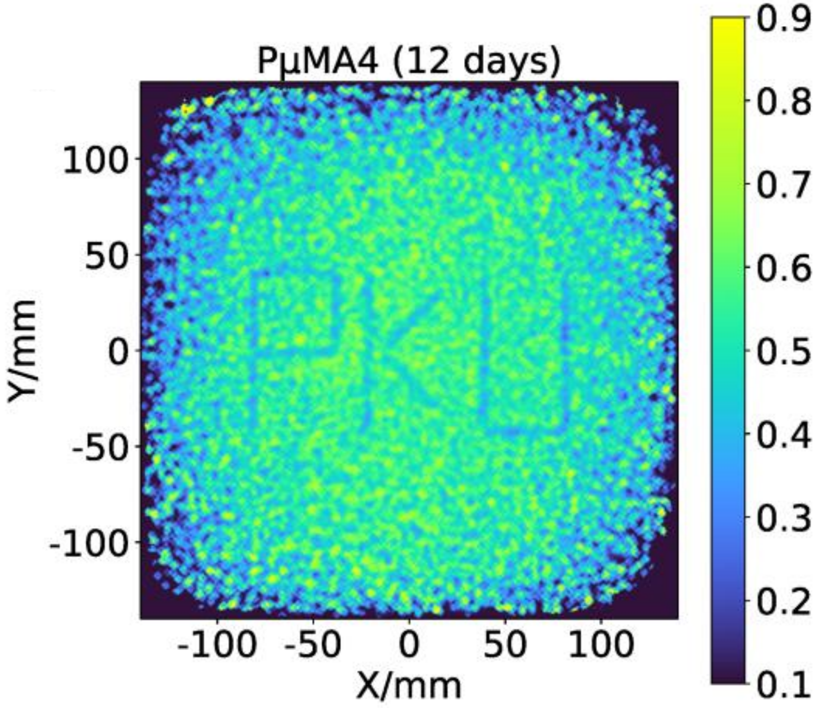

Experimental Results

Experimental Imaging Results 2 -- Gear

How many teeth does my gear have, Mr. Muon?

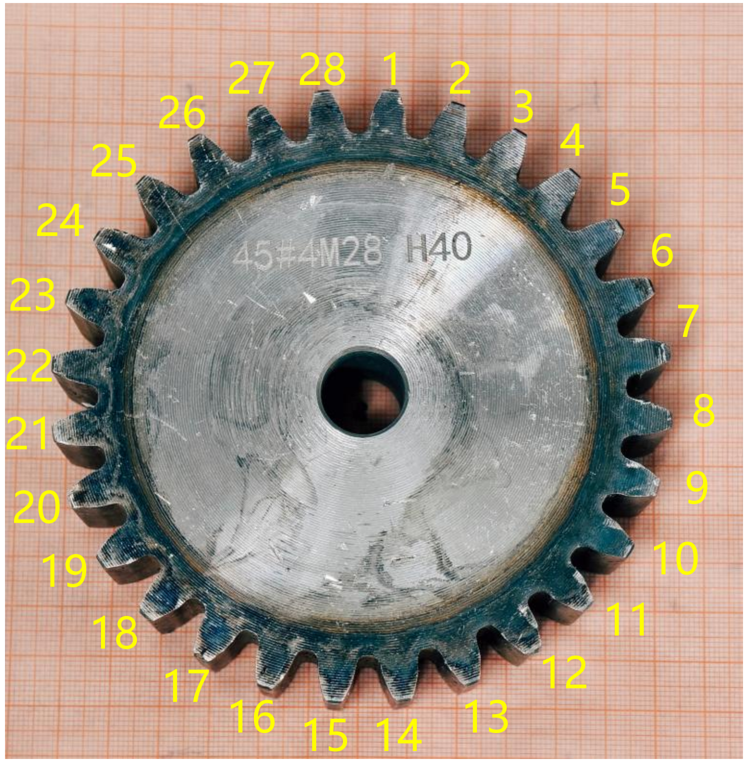

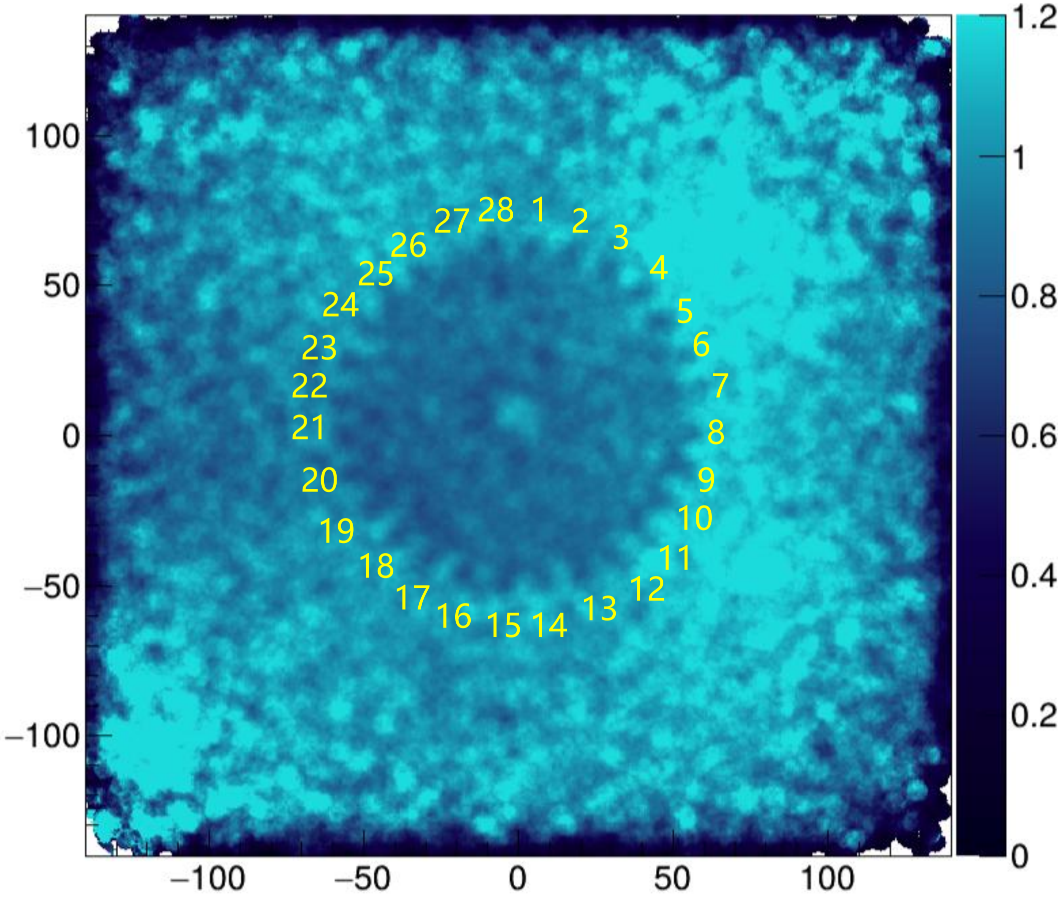

6.5 days

Summary

- We have proposed the PμMA methods, which comprehensively utilize both muon transmission and scattering information, with the simplest configuration requiring only two detector layers.

- In simulated imaging of the air-lead boundary, PμMA produces clear transmission images with sharp edges. From the perspective of edge width metrics, PμMA has a clear advantage over PoCA-based methods. Simulations with monoenergetic collimated beams suggest a higher resolution potential for the PμMA methods.

- Using the RPC setup in our local laboratory, we successfully achieved clear imaging of a 2-mm-wide copper sheet sample engraved with the letters "PKU", and a gear with 28 milimeter-scale teeth.

References

[1] Bonomi, G., Checchia, P., D'Errico, M., Pagano, D. & Saracino, G. Applications of cosmic-ray muons. Prog. Part. Nucl. Phys. 112, 103768 (2020).
[2] Morishima, K. et al. Discovery of a big void in Khufu's Pyramid by observation of cosmic-ray muons. Nature 552, 386–390 (2017).
[3] Alvarez, L. W. et al. Search for Hidden Chambers in the Pyramids. Science 167, 832–839 (1970).
[4] Borozdin, K. et al. Cosmic ray radiography of the damaged cores of the Fukushima reactors. Phys. Rev. Lett. 109, 152501 (2012).
[5] Borozdin, K. N. et al. Radiographic imaging with cosmic-ray muons. Nature 422, 277 (2003).
[6] Yu, P. et al. A new efficient imaging reconstruction method for muon scattering tomography. Nucl. Instrum. Methods Phys. Res., Sect. A 1069, 169932 (2024).
[7] Settles, G.S. Basic Concepts. In Schlieren and Shadowgraph Techniques. 25–38 (Springer Berlin Heidelberg, 2001).
[8] Yu, X. et al. Proposed Peking University muon experiment for muon tomography and dark matter search. Phys. Rev. D 110, 016017 (2024).
[9] Liu, C. et al. Probing cosmic ray composition and muonphilic dark matter via muon tomography. Phys. Rev. Lett. 136, 151001 (2026).
[10] Li, Q. et al. Study of spatial resolution properties of a glass RPC. Nucl. Instrum. Methods Phys. Res., Sect. A 663, 22–25 (2012).
[11] Li, Q. T. et al. A sub-millimeter spatial resolution achieved by a large sized glass RPC. Chin. Phys. C 37, 016002 (2013).
[12] Hagmann, C., Lange, D. & Wright, D. Cosmic-ray shower generator (CRY) for Monte Carlo transport codes. 2007 IEEE Nuclear Science Symposium Conference Record 1143–1146 (IEEE, 2007).
[13] Bethe, H. A. Molière’ s Theory of Multiple Scattering. Phys. Rev. 89, 1256–1266 (1953).
[14] Paulter, N. G., Larson, D. R. & Blair, J. J. The IEEE Standard on Transitions, Pulses, and Related Waveforms, Std-181-2003. IEEE Trans. Instrum. Meas. 53, 1209–1217 (2004).
[15] Maître, H. Image Quality. In From Photon to Pixel(ed. Maître, H.) 205–255 (Wiley, 2017).
[16] Xu, Y. et al. Feasibility study of the GeV-energy muon source based on the High Intensity Heavy-Ion Accelerator Facility. Phys. Rev. Accel. Beams 28, 053401 (2025).
[17] Zhang, F. et al. Proof-of-principle demonstration of muon production with an ultrashort high-intensity laser. Nat. Phys. 21, 1050–1056 (2025).

北京大學 PEKING UNIVERSITY

中国科学院近代物理研究所 Institute of Modern Physics, Chinese Academy of Sciences

中国工程物理研究院

Thank you for listening!

Contributors: Zibo Qin, Rongfeng Zhang, Pei Yu, Cheng-en Liu, Liangwen Chen, Feng Zhang, Zhe Yang, Zaihong Yang, Qite Li, Qiang Li.

Cooperative Partners: Institute of Modern Physics, Chinese Academy of Sciences
National Key Laboratory of Plasma Physics, Laser Fusion Research Center (LFRC), China Academy of Engineering Physics (CAEP)

Introduction-Muon Imaging

Muon Transmission Radiography (MTR)

- Measuring the attenuation of the cosmic-ray muon flux after passing through a target.
- Applied for volcano interior imaging, archaeological structure (e.g., pyramids) scanning, large industrial vessel inspection.
- Rarely ued on small targets.

Search for Hidden Chambers in the Pyramids

The structure of the Second Pyramid of Giza is determined by cosmic-ray absorption.

Luis W. Alvarez, Jared A. Anderson, F. El Bedwei, James Burkhard, Ahmed Fakhry, Adib Girgis, Amr Goneid, Fikhry Hassan, Dennis Iverson, Gerald Lynch, Zenab Miligy, Ali Hilmy Moussa, Mohammed-Sharkawi, Lauren Yazolino

1970, first attempt
(Science 167, 832-839)

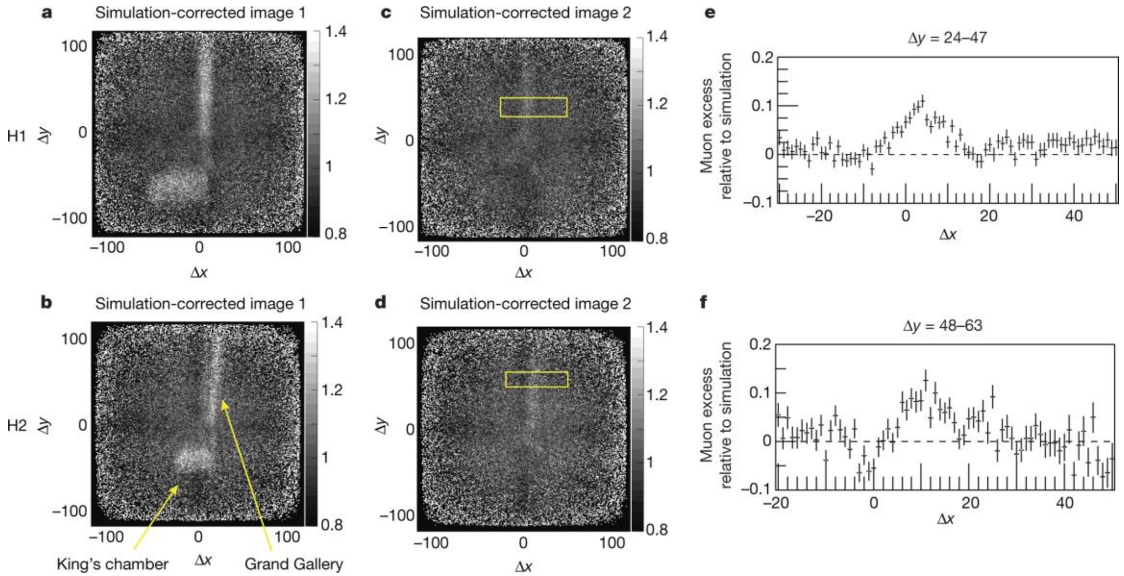

2017, discovery in Khufu's Pyramid
(Nature 552, 386–390)

Introduction-Muon Imaging

Another Example--The Fukushima Reactors

- Practical oriented research.
- Both scattering and transmission methods were used.

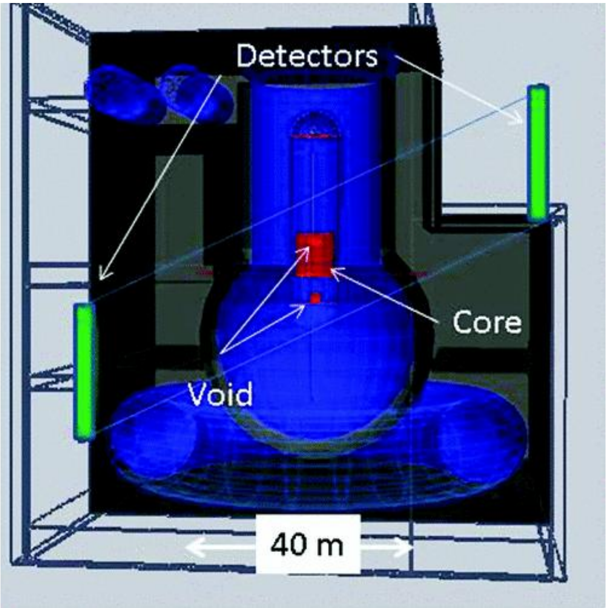

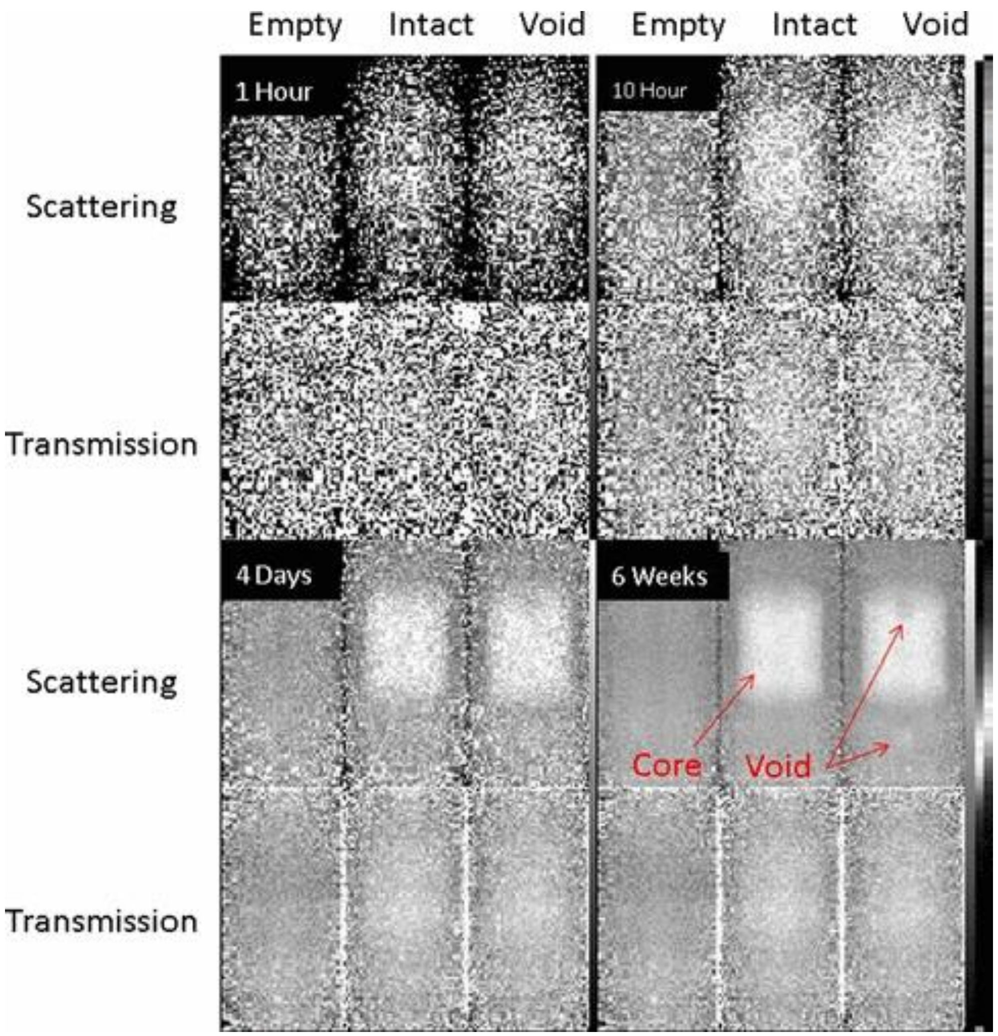

Phys. Rev. Lett. 109, 152501 (2012)

The PμMA Methods-An Analogy

Shadowgraph & Schlieren Photography

Shadowgraph and schlieren photography are optical methods that reveals non-uniformities in transparent media like air, water, or glass. These techniques work by imaging the deflections of light rays that are refracted by a moving fluid, allowing normally unobservable changes in a fluid's refractive index to be seen.

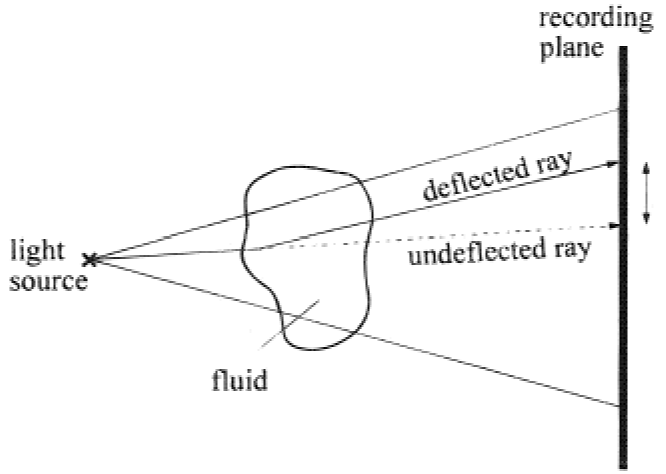

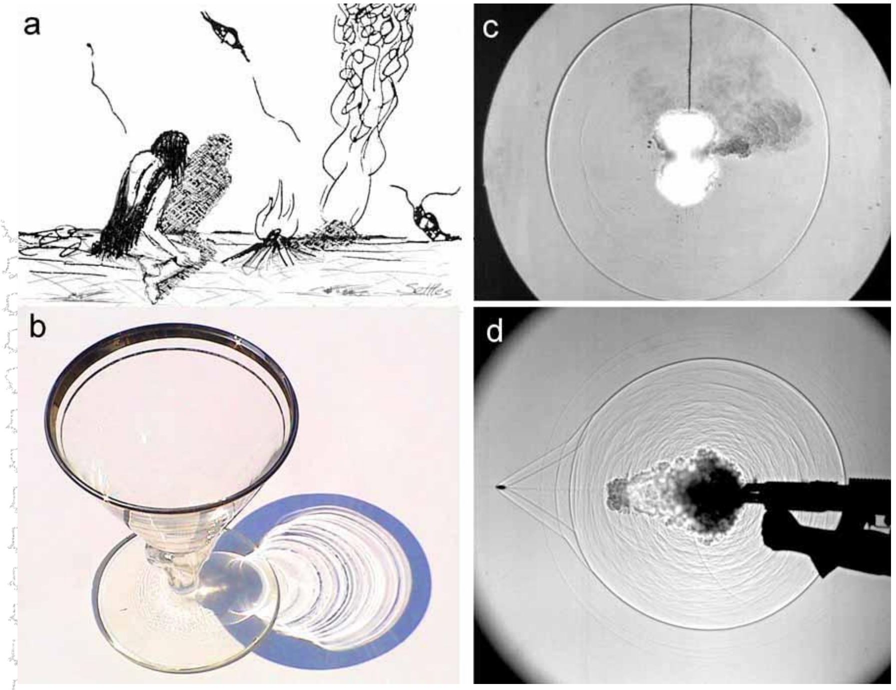

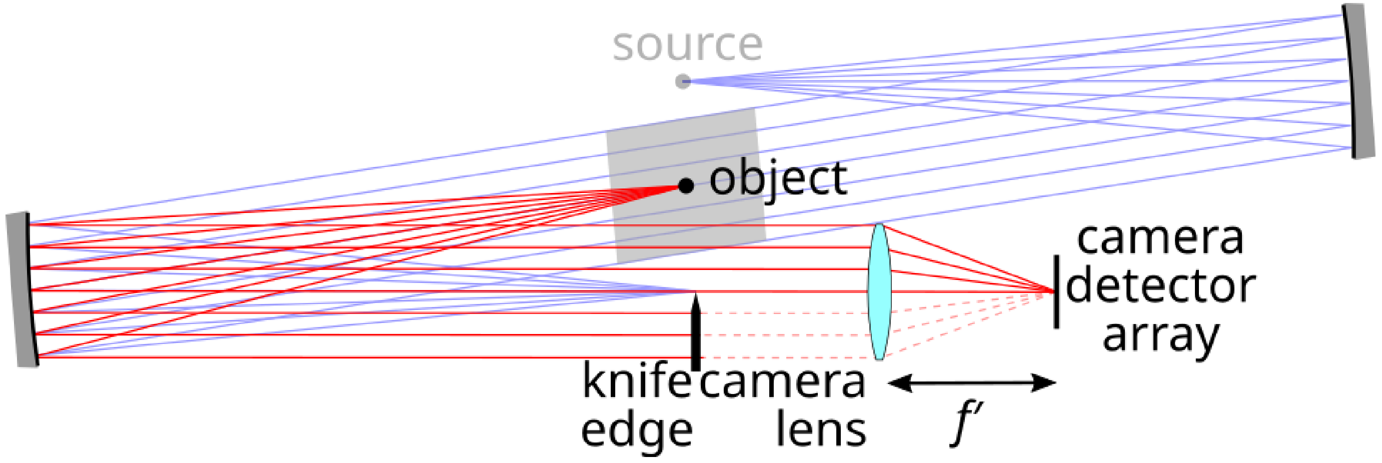

The PμMA Methods-Muon "Shadowgraph"

PμMA as a Shadowgraph

The PμMA methods share similarities with optical shadowgraph (or Schlieren) imaging. However, the two techniques differ in implementation due to several factors:

-the causes of particle/ray deflection are different;

-the scattering angle of muons follows the statistical distribution of multiple Coulomb scattering, whereas the refraction of light obeys Snell's law;

$$\sigma_\theta = \frac{13.6\mathrm{MeV}}{\beta c p} z \sqrt{\frac{x}{X_0}} \left[1 + 0.038 \ln\left(\frac{x z^2}{X_0 \beta^2}\right)\right]$$

-cosmic-ray muons have a low flux and cannot be collimated;

-the position resolution of muon detectors is lower than that of optical cameras.

Imaging Results & Evaluation

Areal Density Response

PμMA methods are sensitive to the areal density of different regions in a sample, and this sensitivity can be used to differentiate between regions of varying areal density.

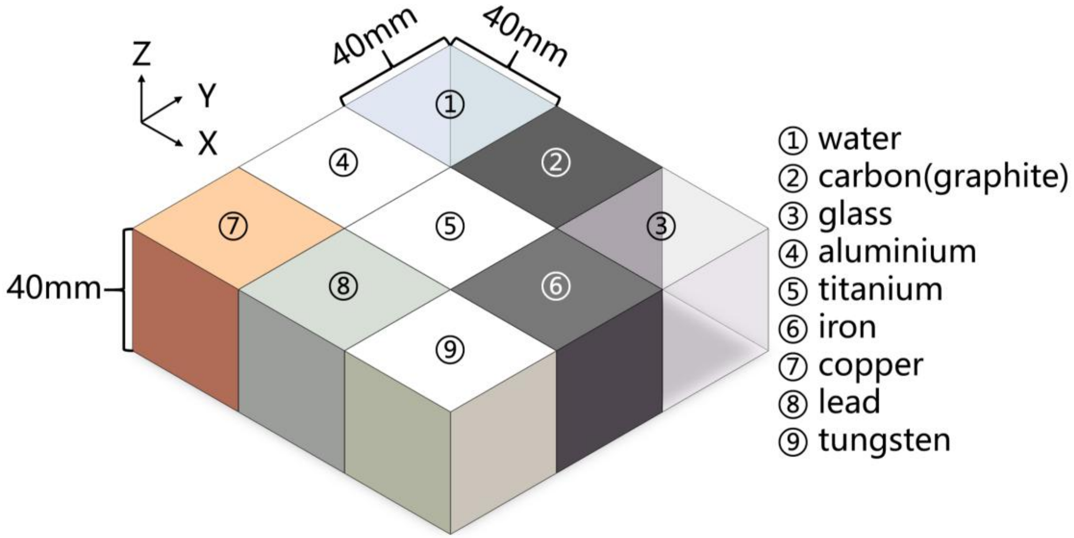

Nine types of samples, each measuring 40×40×40 mm, closely arranged.

Approximately 10 million events.

Imaging Results & Evaluation

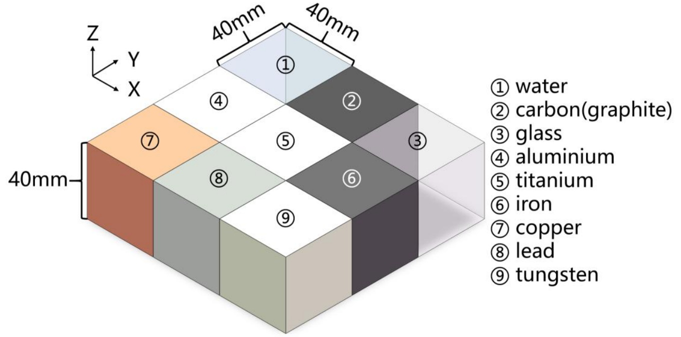

Areal Density Response

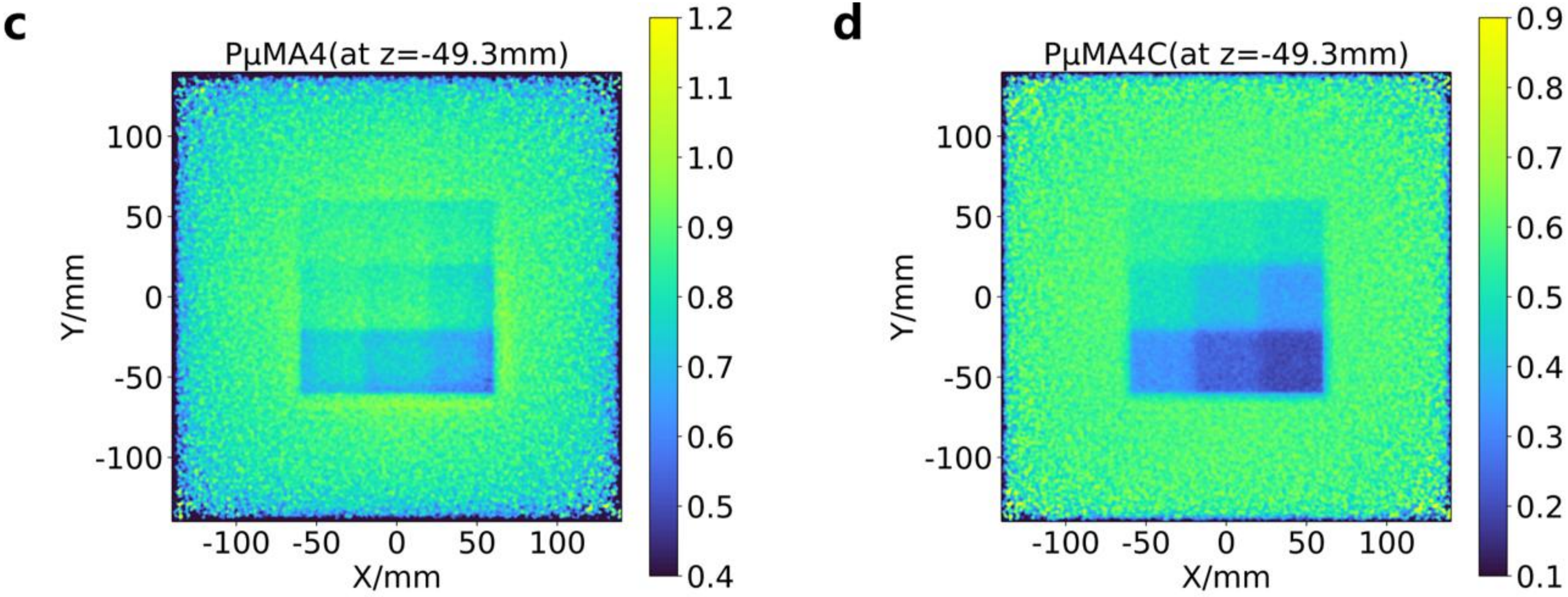

Imaging Results & Evaluation

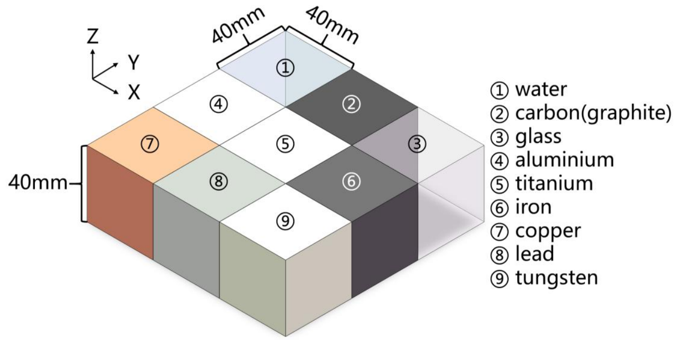

Areal Density Response

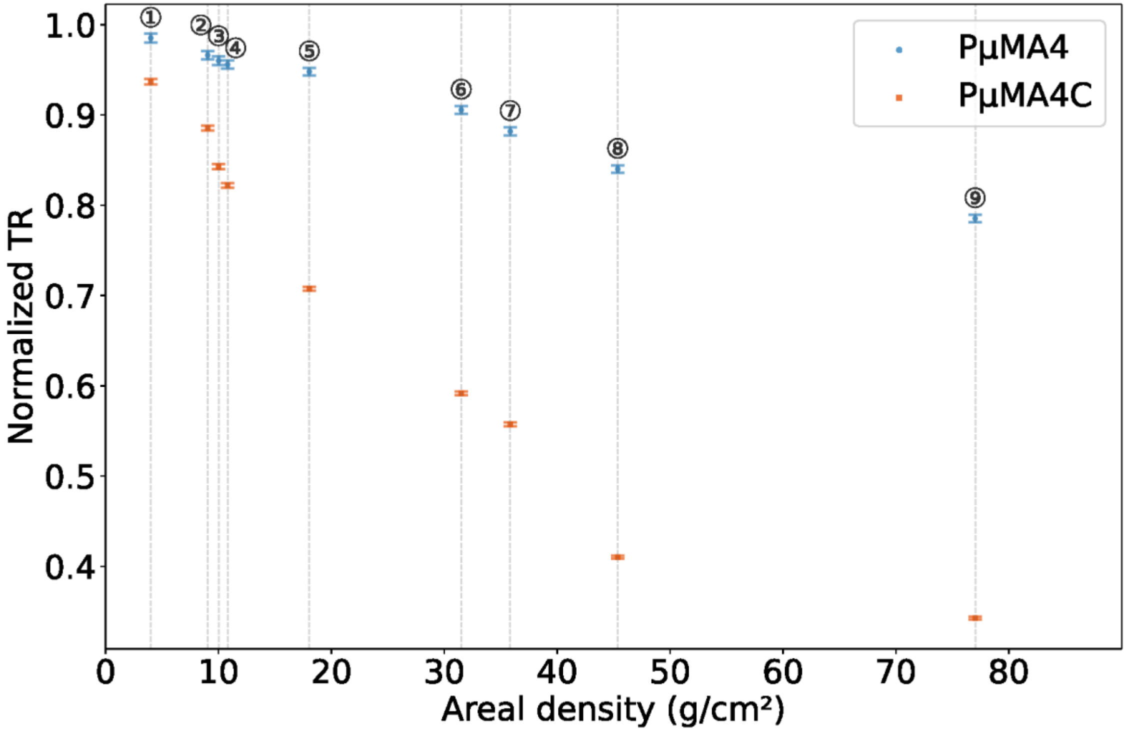

PμMAC methods demonstrate stronger capability in distinguishing regional areal densities.